

<sup>1</sup>Current Address: Department of Physics, Boston University, Boston, MA 02215  
<sup>2</sup>Current Address: Center for Astrophysics, 60 Garden St. Cambridge, MA 02138

Classical non-topological soliton configurations are considered within the theory of a complex scalar field with a gauged  $U(1)$  symmetry. Their existence and stability against dispersion are demonstrated and some of their properties are investigated analytically and numerically. The soliton configuration is such that inside the soliton the local  $U(1)$  symmetry is broken, the gauge field becomes massive and for a range of values of the coupling constants the soliton becomes a superconductor pushing the charge to the surface. Furthermore, because of the repulsive Coulomb force, there is a maximum size for these objects, making impossible the existence of  $Q$ -matter in bulk form. We also briefly discuss solitons with fermions in a  $U(1)$  gauge theory.

Abstract

<sup>a</sup>Theoretical Physics Group  
Fermi National Accelerator Laboratory  
P.O. Box 500, Batavia, IL 60510  
<sup>b</sup>NASA/Fermilab Astrophysics Center  
Fermi National Accelerator Laboratory  
P.O. Box 500, Batavia, IL 60510  
<sup>c</sup>Department of Physics  
University of California  
Santa Barbara, CA 93106  
<sup>d</sup>Department of Physics  
The University of Chicago  
Chicago, IL 60637

Kimyeong Lee<sup>a,1</sup>, Jaime A. Stein-Schabes<sup>b</sup>,  
Richard Watkins<sup>c</sup>, Lawrence M. Widrow<sup>b,d,2</sup>

Gauged Q-Balls

FERMILAB-Pub-88/139-A  
September 30, 1988

Fermi National Accelerator Laboratory



N89-11500

(FERMI 204  
CSCL 204)

(NASA-CR-183369) GAUGE Q-BALLS  
NATIONAL ACCELERATOR LAB.) 45 P

Unclas  
G3/72 C170072

ORIGINAL PAGE IS  
OF POOR QUALITY



## 1 Introduction

Non-topological solitons (NTSs) are extended objects that arise in theories with unbroken global symmetries [1,2]. The simplest example of a NTS is the so-called Q-ball that can appear in a  $U(1)$ -invariant theory with a single complex scalar field  $\phi$  that has non-linear self-interactions [1,3,4]. The results for Q-balls found in the literature may be applicable to models that possess an unbroken global  $U(1)$  symmetry such as  $B - L$ . In this paper we study the properties of Q-balls in a local or gauged  $U(1)$  theory. Our work is a first step in understanding how NTSs might arise in gauge theories such as electromagnetism, the Weinberg-Salam model, or Grand Unified Theories (e.g.,  $SU(5)$ ,  $SO(10)$ ,  $E_6$ ).

A NTS is a non-dissipative solution to the classical field equations that, for fixed charge  $Q$ , represents the field configuration with the lowest energy. For the Q-ball, the basic structure is very simple. Outside the Q-ball,  $U(1)$  is unbroken and  $\phi$  particles have mass  $\mu$  (this is the true vacuum of the theory). Inside the Q-ball,  $U(1)$  is broken and a condensate of the  $\phi$  field forms with an energy per unit charge less than  $\mu$ . Furthermore, the time-dependence of the  $\phi$  field gives rise to a non-zero charge density. The negative pressure of the false vacuum interior is balanced by the positive pressure from the confined  $\phi$  particles (for possible creation mechanisms see [5]).

Coupling of  $\phi$  to a  $U(1)$  gauge field leads to two basic effects. 1) Inside the Q-ball, the  $U(1)$  symmetry is broken and the gauge field has a mass  $m_V$ . For Q-balls that are large compared to the Compton wavelength of the gauge field ( $\xi = m_V^{-1}$ ), the charge is pushed to the surface of the Q-ball and the characteristic width of the shell in which most of the charge resides is  $O(m_V^{-1})$ . It is in this limit that the Q-ball becomes *superconducting*. For small Q-balls, the charge is only slightly enhanced near the surface. These results are a clear signal that the Q-ball is behaving like a lump of superconducting matter (which it must since  $U(1)$  is broken inside the Q-ball). 2) Gauged Q-balls can only be so big.

For small enough values of the charge  $Q$  and gauge coupling  $e$ , the 'electrostatic' energy of the Q-ball [ $=O(e^2 Q^2/R)$ ] is smaller than the other energies in the problem and therefore we expect stable gauged Q-balls to exist. Suppose we fix  $e$  but slowly increase  $Q$  by bringing charges (i.e., free  $\phi$  particles) to the surface of the Q-ball from very far away. For some value of  $Q$  ( $\equiv Q_{max}$ ) the cost in Coulomb energy for adding an extra unit of

charge becomes greater than the energy gained by bringing it from the true vacuum to the false vacuum. From this point on it becomes energetically favorable to leave additional charges as free  $\phi$  particles. A corollary of this result is that for large enough values of  $e$  there are no stable Q-balls. As will be discussed below, very small Q-balls are unstable and evaporate into free particles. Therefore, stable Q-balls must have charge greater than some value  $Q_{min}$ . If  $Q_{max} < Q_{min}$  then there are no stable Q-balls.

The fact that there is a maximum value for the allowed charge of a gauged Q-ball points to a fundamental difference with the ungauged ( $e = 0$ ) case. In the  $e = 0$  case, it is possible to have bulk Q-matter occupying an arbitrarily large region of space. This is impossible in the gauged case.

An outline of the paper is as follows: In Section II we describe the particle physics setting for gauged Q-balls. We review the basic properties of ordinary ( $e = 0$ ) Q-balls and derive some general properties of gauged Q-balls. In Section III, we study gauged Q-balls using trial functions for the fields. The calculations are carried out for thin shell Q-balls and ones in which the gauge coupling and charge are assumed to be small. [How small will be made explicit below.] Section IV is devoted to numerical results. The equations of motion are numerically integrated on computer and some solutions are obtained. When appropriate, these results are compared with the analytic results obtained in the preceding sections. In Section V we consider solitons with fermions that are coupled to a  $U(1)$  gauge field. Finally, in Section VI, we summarize and discuss our results.

## 2 General Setting

Consider a complex scalar field  $\phi(\vec{r}, t) = f(\vec{r}, t) \exp(i\theta(\vec{r}, t)) / \sqrt{2}$  coupled to a  $U(1)$  gauge field  $A_\mu$ . The Lagrange density for the theory is

$$\mathcal{L} = \frac{1}{2} \partial_\mu f \partial^\mu f + \frac{1}{2} f^2 (\partial_\mu \theta - e A_\mu)^2 - U(f) - \frac{1}{4} F_{\mu\nu} F^{\mu\nu} \quad (2.1)$$

where  $F_{\mu\nu} = \partial_\mu A_\nu - \partial_\nu A_\mu$  and  $U(f)$  is the  $U(1)$ -invariant scalar potential. [For definiteness, we take  $e > 0$ .] The conserved charge associated with the  $U(1)$  symmetry is

$$Q = \int d^3r f^2 (\dot{\theta} - e A_0) \quad (2.2)$$

where the dot means  $d/dt$ . For definiteness, we shall take  $Q$  to be positive.

We begin by reviewing the basic properties of ordinary ( $e = 0$ ) Q-balls. We assume that in the true vacuum  $U(1)$  is unbroken, so that the absolute minimum of the potential  $U(f)$  occurs at  $f = 0$ . The mass  $\mu$  of a free  $\phi$  particle is given by

$$\mu^2 \equiv \left. \frac{d^2 U}{df^2} \right|_{f=0}. \quad (2.3)$$

A necessary condition [4] for the existence of Q-balls is that

$$\omega_o^2 = \min \left( \frac{2U(f)}{f^2} \right) \quad (2.4)$$

for some  $f = F_o$  with  $F_o$  finite and non-zero and  $0 < \omega_o < \mu$ . For large enough  $Q$ , the lowest energy state is a coherent configuration of the boson field  $\phi$  confined to a finite spatial region. Following Coleman[4], we refer to this object as a Q-ball.

In order for a Q-ball to be stable against dispersion into free particles, its energy must be less than the energy of  $Q$  free particles. Consider a field configuration where inside some volume  $V$ ,  $f$  has a constant value  $F$  and  $\theta = \omega t + \theta_o$  where  $\theta_o$  is a disposable constant. Outside of  $V$ ,  $f = 0$ . For large enough  $V$  (or  $Q$ ) we can neglect the surface energies and treat  $f$  as a step function at the boundary of  $V$ . The total conserved charge, which characterizes the system, is  $Q = \omega F^2 V$ . The total energy is then

$$E = \frac{Q^2}{2F^2 V} + U(F)V. \quad (2.5)$$

We minimize the energy with respect to  $V$  and find that

$$V = \frac{Q}{\sqrt{2F^2 U(F)}} \quad (2.6)$$

and so the energy becomes

$$E = Q \sqrt{\frac{2U(F)}{F^2}}. \quad (2.7)$$

Next, we minimize  $E$  with respect to  $F$  keeping  $Q$  fixed and find that  $F = F_o$  (cf. Eqn.(2.4)). For  $F = F_o$ , the energy of the Q-ball is  $E = \omega_o Q$ . With  $\omega_o < \mu$ , the Q-ball has lower energy than the energy of  $Q$  free particles and is therefore stable against dispersion. The negative vacuum pressure  $-U(F_o)$  is balanced by the positive 'kinetic'

pressure,  $\omega_o F_o^2/2$ . Assuming that there is no further complexity in the potential (e.g. coupling of  $\phi$  to light fermions [6]), Q-balls will be absolutely stable.

The result  $E = \omega_o Q$  is valid only for very large Q-balls. For small Q-balls where surface energies are important,  $E$  can be much larger than  $\omega_o Q$  and can in fact be larger than  $\mu Q$ . In general there is a lower bound on the allowed values of  $Q$  for stable Q-balls. However, even for a large Q-ball, the surface energy is important as it determines the shape of the configuration. Since the surface energy is minimized by choosing, for a fixed volume, the shape with the smallest surface area, the groundstate Q-ball is a sphere.

We now consider gauged  $U(1)$  Q-balls ( $e \neq 0$ ) where  $\phi$  is coupled to the gauge field  $A_\mu$  as in Eqn.(2.1). One expects gauged Q-balls to be stable as long as their electrostatic self-energy is much smaller than the other energies. As before,  $f$  is non-zero and  $U(1)$  is broken inside the Q-ball. As a consequence of the symmetry breaking, the gauge field is massive inside and the Q-ball is a  $U(1)$  superconductor.

Consider a coherent configuration of  $\phi$  and  $A_\mu$  with a given electric charge  $eQ$ . The lowest energy state will have no 'electric' currents and therefore no magnetic field. Furthermore, the lowest energy configuration will be spherically symmetric and stationary. For this configuration one can choose a gauge such that  $\theta = \omega t$  ( $\theta_o = 0$ ) with  $\omega$  constant and  $A_o(r) \rightarrow 0$  as  $r \rightarrow \infty$  where  $r \equiv |\vec{r}|$ . For definiteness, we assume that  $\omega > 0$ . The spatial components of the gauge potential are zero as there is no magnetic field. With the exception of  $\theta$ , the fields are time independent.

The Lagrangian for the configuration described above is

$$L = 4\pi \int r^2 dr \left[ -\frac{1}{2} f'^2 + \frac{1}{2e^2} g'^2 + \frac{1}{2} f^2 g^2 - U(f) \right] \quad (2.8)$$

where  $g(r) = \omega - eA_o(r)$  and prime denotes  $d/dr$ . By varying  $L$  with respect to  $f$  and  $g$  at fixed  $\omega$  we find the equations of motion:

$$f'' + \frac{2}{r} f' + f g^2 - dU(f)/df = 0 \quad (2.9)$$

$$g'' + \frac{2}{r} g' - e^2 f^2 g = 0. \quad (2.10)$$

The total energy and charge are given by

$$E = 4\pi \int r^2 dr \left[ \frac{1}{2} f'^2 + \frac{1}{2e^2} g'^2 + \frac{1}{2} f^2 g^2 + U(f) \right] \quad (2.11)$$

$$Q = 4\pi \int r^2 dr f^2 g \quad (2.12)$$

Eqn.(2.10) was derived by varying  $L$  with respect to  $A_0$ . Since  $\dot{A}_0$  does not appear in the Lagrangian, we must treat Eqn.(2.10) as a constraint equation rather than a dynamical one. Eqn.(2.9) can be obtained by varying the energy in Eqn.(2.11) with respect to  $f$  under the constraint Eqn.(2.10).

Some qualitative features of the soliton solutions are readily apparent. From Eqns.(2.10, 2.12) we see that

$$e^2 Q = \lim_{r \rightarrow \infty} 4\pi r^2 g'. \quad (2.13)$$

For large  $r$ ,  $g \rightarrow \omega - e^2 Q / 4\pi r$ ,  $f$  is small and  $U(f) \simeq \mu^2 f^2 / 2$ . Eqn.(2.9) then becomes

$$f'' + \frac{2}{r} f' + (g^2 - \mu^2) f = 0 \quad (2.14)$$

and  $f \propto \exp(-r\sqrt{\mu^2 - \omega^2})/r$ . For the existence of a localized solution without oscillations we require  $\omega < \mu$ . Additionally, for the solution to be well behaved at the origin,  $f'(r)$  and  $g'(r)$  should approach zero at least faster than  $r$  for  $r \rightarrow 0$ .

We now show that  $g(r)$  obeys the following inequalities:

$$0 < g(0) \leq g(r) \leq g(\infty) = \omega < \mu. \quad (2.15)$$

It is convenient to write Eqn.(2.10) in the following form:

$$(r^2 g')' = e^2 r^2 f^2 g. \quad (2.16)$$

We will first prove that  $g(0) > 0$ . Suppose that  $g(0) = 0$ . Since  $g'(0) = 0$ , then  $g(r)$  would be zero for all  $r$ . Suppose instead that  $g(0) < 0$ . Eqn.(2.10) then implies that  $r^2 g'$  is a decreasing function of  $r$  so that  $g'(r)$  goes negative and  $g(r) < 0$  for all  $r$ . Neither of these possibilities are acceptable given that  $\omega > 0$  and  $g(r) \rightarrow \omega$  for  $r \rightarrow \infty$ . The only acceptable possibility is that  $g(0) > 0$ . We then see that  $g'(r)$  is positive and therefore  $g(r)$  is a monotonically increasing function of  $r$ .

Let us consider a different form of the energy integral. After partial differentiation and using the asymptotic behavior of  $f$  and  $g$ , Eqns.(2.11,2.12) lead to the new energy functional

$$E = \frac{1}{2} \omega Q + 4\pi \int dr r^2 \left[ \frac{1}{2} f'^2 + U(f) \right] \quad (2.17)$$

ORIGINAL PAGE IS  
OF POOR QUALITY

where the constraint Eqn.(2.10) is satisfied. Eqn.(2.9) need not be satisfied. However, the energy is minimized by choosing  $f$  to be a solution of Eqn.(2.9).

Demanding that the Lagrangian (2.8) for the solution is stationary at  $\kappa = 1$  under scaling of the form  $r \rightarrow \kappa r$  leads to the following relation

$$\int dr r^2 \left[ -\frac{1}{2} f'^2 + \frac{1}{2e^2} g'^2 \right] + 3 \int dr r^2 \left[ \frac{1}{2} f^2 g^2 - U(f) \right] = 0. \quad (2.18)$$

When used together with Eqns.(2.9-2.12) and the asymptotic forms for  $f$  and  $g$ , the energy can be rewritten as

$$E = \omega Q + \frac{4\pi}{3} \int dr r^2 [f'^2 - g'^2]. \quad (2.19)$$

Consider the case  $e = 0$ , so that  $g' = 0$ . In the thin wall approximation we can neglect the gradient  $f'^2$  term. We then see that  $E = \omega Q$ . It follows that for thin shell Q-balls with  $e \neq 0$  the energy is generally bounded from above by  $\omega Q$  and is less than  $\mu Q$  if  $\omega < \mu$ .

Recall that our goal is to find the lowest energy configuration for a given value of the charge  $Q$ . One possibility is to have  $Q$  free particles of mass  $\mu$ , the total configuration having mass  $\mu Q$ . A second possibility is to have a soliton with charge  $Q$ . In this case, the energy is a very complicated function of the charge. For  $e = 0$  we know that  $E \rightarrow \omega_o Q$  for large  $Q$  so that for  $\omega_o < \mu$  this configuration is favored over the free particle one. For  $e \neq 0$ , we expect that the energy will be increased over the  $e = 0$  case due to Coulomb repulsion with Coulomb energy becoming more important as  $Q$  gets large. For  $\partial E / \partial Q > \mu$  we must consider a third possibility, namely that some of the charge can be put into the Q-ball and some can be put in free particles. Suppose that there exists a  $Q$  ( $\equiv Q_{max}$ ) such that for  $Q > Q_{max}$ ,  $\partial E / \partial Q \geq \mu$  while  $\partial E / \partial Q < \mu$  for  $Q < Q_{max}$ . For  $Q > Q_{max}$ , a Q-ball with charge  $Q_{max}$  plus  $Q - Q_{max}$  free particles will be the lowest energy state for the system.

As discussed above, in very small Q-balls surface energies are important and the Q-balls are generally unstable and disperse into free particles. There is therefore a minimum value allowed for the charge which we define to be  $Q_{min}$ . If the gauge coupling is large enough,  $Q_{max}$  will be less than  $Q_{min}$ , and there will be no stable Q-balls



Clearly, in order to understand gauged Q-balls, we need to determine  $E$  as a function of  $Q$ . We can do this analytically, but only in the thin wall approximation (i.e., neglecting surface energies) and for small values of  $e$  and  $Q$ . On the other hand, we can obtain better results numerically. The results obtained from these two approaches are presented in Sections III and IV respectively.

### 3 Thin Wall Approximation

In this section, we study properties of gauged Q-balls by considering trial functions for the fields. More specifically, we choose a simple trial function for the field  $f$  and solve for  $A_0$  (or equivalently,  $g$ ) using the constraint Eqn.(2.10). These functions can be thought of as an initial configuration for the Q-ball, and will in general have greater energy than the true groundstate configuration. [Recall that for the true groundstate configuration, the fields satisfy their equations of motion, Eqns.(2.9,2.10).] As we shall see in the next section, for a certain range of parameters, the trial functions used here closely approximate the actual solutions.

We choose  $f$  to have a constant value  $F$  inside a sphere of radius  $R$  and zero outside. In real solitons,  $f$  changes continuously from  $F$  to 0 within a shell of some finite width  $T$ . For large Q-balls (width of the shell much less than the radius of the Q-ball) the energy associated with the shell is negligible (the shell energy is of order  $T/R$  of the total energy). In this limit we can treat  $f$  as a step function and discard the  $f'^2$  term in the energy density. This is the thin wall approximation.  $A_0$  or equivalently  $g$  must be determined by solving the constraint Eqn.(2.10). We find that

$$g(r) = \begin{cases} [\omega - e^2 Q/4\pi R] R \sinh(eFr)/r \sinh(eFR) & r \leq R \\ [\omega - e^2 Q/4\pi r] & r > R \end{cases} \quad (3.1)$$

where the gauge is chosen so that  $A_0 \rightarrow 0$  for  $r \rightarrow \infty$ . The system is now determined by four parameters,  $\omega$ ,  $Q$ ,  $F$ , and  $R$ . In the following, we will determine the values for  $\omega$ ,  $F$ , and  $R$  that minimize the energy given a fixed  $Q$ .

Eqn.(2.12) for the charge gives one relation among these four parameters:

$$\omega = \frac{e^2 Q}{4\pi R} \left[ 1 - \frac{\tanh x}{x} \right]^{-1} \quad (3.2)$$

ORIGINAL PAGE IS  
OF POOR QUALITY

where  $x = eFR$ . We can use this expression to eliminate  $\omega$  from  $E$  in Eqn.(2.17).

$$E = \frac{e^2 Q^2}{8\pi R} \left[ 1 - \frac{\tanh x}{x} \right]^{-1} + \frac{4\pi}{3} R^3 U(F) \quad (3.3)$$

Minimizing the energy with respect to  $R$  (or  $x$ ) for fixed  $Q$  and  $F$  gives an expression for  $x$  in terms of  $Q$  and  $F$ :

$$x \left[ \frac{x}{\tanh x} - 1 \right] = \frac{e^3 Q F^2}{4\pi \sqrt{2U(F)}}. \quad (3.4)$$

In principle, one can use this expression to eliminate  $R$  (and  $x$ ) from the expression for the energy. The result would be an expression for the energy in terms of  $Q$  and  $F$ . The final steps are to minimize the energy with respect to  $F$  for fixed  $Q$  and to then eliminate  $F$ . The result is the desired expression for  $E$  in terms of  $Q$ .

Unfortunately, Eqn.(3.4) is a transcendental equation for  $R$  in terms of  $Q$  and  $F$  and exact results from this point on are difficult if not impossible to obtain. We can however, carry out the above steps for the case where  $x \ll 1$ . As we shall see,  $x \ll 1$  implies that the Coulomb energy is small compared to the potential and kinetic energies. In this regime, the radius and total energy of the groundstate Q-ball differ from the  $e = 0$  case by terms of order  $x^2$ . We now proceed to calculate these corrections.

For small  $x$ , Eqn.(3.4) becomes

$$x^3 \left( 1 - \frac{x^2}{15} \right) = e^3 Q C \quad (3.5)$$

or

$$R = \left( \frac{3Q}{4\pi F \sqrt{2U(F)}} \right)^{1/3} \left( 1 + \frac{e^2 Q^{2/3} C^{2/3}}{45} \right) \quad (3.6)$$

where  $C \equiv 3F(F^2/2U(F))^{1/2}/4\pi$ . For most of the potentials that we will consider,  $C$  is of order unity. Our expansion is therefore valid for  $x^2$ . Note that when  $e = 0$  we recover the result for the radius of ordinary Q-balls (Eqn.(2.6) with  $V = 4\pi R^3/3$ ).

We can use Eqns.(3.5,3.6) to eliminate  $x$  and  $R$  from Eqn.(3.3) to obtain

$$E = Q \sqrt{\frac{2U(F)}{F^2}} \left( 1 + \frac{e^2 Q^{2/3} C^{2/3}}{5} \right). \quad (3.7)$$

Again, when  $e$  is set to zero we recover the result for the energy of ordinary Q-balls, Eqn.(2.7).

Let us assume that the function  $U/F^2$  is minimized by choosing  $F = F_o$  (cf. Eqn.(2.4) in the case where  $e = 0$ ). The energy in Eqn.(3.7) is minimized for  $F = F_o(1 - \Lambda)$  where

$$\Lambda \equiv \frac{e^2}{5} \left( \frac{2Q^2 \omega_o^4}{3\pi^2 F_o^4} \right)^{1/3} \left( \left[ \frac{\partial^2}{\partial F^2} \left( \frac{U(F)}{F^2} \right) \right]_{F=F_o} \right)^{-1} \quad (3.8)$$

In deriving Eqn.(3.8) we have made use of the fact that  $\partial(U/F^2)/\partial F = 0$  when evaluated at  $F = F_o$ . By substituting  $F = F_o(1 - \Lambda)$  into Eqn.(3.7) we obtain the desired expression for  $E$  in terms of  $Q$ . Likewise, we can use Eqn.(3.8) together with Eqn.(3.6) to find  $R = R(Q)$ . Eqn.(3.7) can be put into the following suggestive form:

$$E = Q \sqrt{\frac{2U(F)}{F^2}} + \frac{3e^2 Q^2}{20\pi R}. \quad (3.9)$$

The first term is the energy of the Q-ball neglecting gauge interactions. The second term is the electrostatic self-energy of the Q-ball, with  $e^2 Q^2/8\pi R$  being the electrostatic energy in the region  $r > R$  and  $e^2 Q^2/40\pi R$  the electrostatic energy for  $r < R$ . Also in the small  $x$  approximation the first term is the leading order term. The second term is  $O(x^2)$ .

In order to better understand the above results, we consider the following form for the potential:

$$U(f) = \frac{\lambda^2 f^6}{6\mu^2} - \frac{f^4}{4} + \frac{\mu^2 f^2}{2}. \quad (3.10)$$

where  $\lambda$  is a dimensionless constant and  $\mu$  is again the mass of a free  $\phi$  particle. We require that  $\lambda^2 > 3/16$  so that  $U(f) > 0$  for all  $f \neq 0$ . As discussed above, a necessary condition for the existence of Q-balls is that the function  $U(f)/f^2$  has a minimum for some non-zero  $f$ . [It is for this reason that we must consider sixth (or higher) order potentials.] This is always true for the above potential and the minimum occurs at  $F_o = \sqrt{3}\mu/2\lambda$ . Note that the existence of Q-balls does not depend on the metastable false vacuum which exists when  $\lambda^2 < 1/4$ .

For ordinary ( $e = 0$ ) Q-balls with an effective potential for  $\phi$  described by Eqn.(3.10), we get

$$E = \mu\alpha Q \quad (3.11)$$

where  $\alpha = (1 - 3/16\lambda^2)^{1/2} = \omega_o/\mu$ . Indeed, this energy is less than  $\mu Q$ , the energy of  $Q$  free  $\phi$  particles. The energy gained by bringing a single  $\phi$  particle from the true vacuum to the false vacuum is just  $\mu[1 - \alpha]$ .

Given the potential, we can readily evaluate the quantities discussed above. We find that

$$\Lambda = \frac{2}{15} \left( \frac{e^3 Q \lambda^2 \alpha^2}{\pi} \right)^{2/3}. \quad (3.12)$$

The energy in terms of  $Q$  is given by

$$E = \mu \alpha Q \left[ 1 + \frac{3}{20} \left( \frac{e^3 Q}{\pi \lambda \alpha} \right)^{2/3} \right]. \quad (3.13)$$

Finally, the radius is given by

$$R = \left( \frac{\lambda^2}{\pi} \right)^{1/3} \frac{Q^{1/3}}{\mu \alpha^{1/3}} \left[ 1 + \frac{4}{45} \left( \frac{\lambda^2 e^3 Q}{\pi \alpha} \right)^{2/3} \right]. \quad (3.14)$$

For a given charge  $Q$ , we see that both the radius and the energy are larger in the gauged case than in the  $e = 0$  case.

Let us now determine  $Q_{max}$ , the maximum allowable charge for stable gauged Q-balls. From Eqn.(3.13), we find that

$$\frac{\partial E}{\partial Q} = \mu \alpha \left[ 1 + \frac{1}{4} \left( \frac{e^3 Q}{\pi \lambda \alpha} \right)^{2/3} \right]. \quad (3.15)$$

We solve for  $Q_{max}$  by setting this equal to  $\mu$ :

$$Q_{max} = \frac{8\pi\lambda}{e^3\alpha^{1/2}} (1 - \alpha)^{3/2}. \quad (3.16)$$

Using Eqn.(3.14), we can rewrite this expression in a more transparent form:

$$\frac{e^2 Q_{max}}{4\pi R} = \mu [1 - \alpha] \quad (3.17)$$

The left-hand side is just the cost in energy due to Coulomb-type forces for bringing a particle to the surface of the Q-ball from very far away. The right hand side is the energy gained (when the Coulomb energy is neglected) in bringing a particle from the true vacuum into the false vacuum Q-ball interior. As stated above, and verified by Eqn.(3.17),  $Q_{max}$  defines the value of  $Q$  where it becomes energetically favorable to keep additional charges outside and far away from the Q-ball.

Of course Eqns.(3.12-3.17) are valid only when  $x$  is small. Recall that to leading order

$$x^3 = \frac{3e^3 Q F}{4\pi} \left( \frac{F^2}{2U(F)} \right)^{1/2}. \quad (3.18)$$

For the potential Eqn.(3.10), we have that

$$x^3 = \frac{3\sqrt{3}e^3Q}{8\pi\lambda\alpha} \quad (3.19)$$

At  $Q = Q_{max}$ ,  $x = [3(1-\alpha)/\alpha]^{1/2}$ . It therefore follows that  $x < 1$  for  $\alpha > 3/4$  or  $\lambda^2 > 3/7$ .

From Eqns. (3.16) and (3.17) we can get the maximum radius for this configuration,

$$R_{max} = \frac{2\lambda}{\mu e} \sqrt{\frac{1-\alpha}{\alpha}}. \quad (3.20)$$

In order to interpret the breaking of the  $U(1)$  symmetry inside the Q-ball as superconductivity, we need to compare the  $R_{max}$  with the penetration length  $\xi$  associated with the mass of the photon (or equivalently, the Compton wavelength of the gauge field in a region where the  $U(1)$  symmetry is broken). We find that

$$\xi = \frac{1}{m_V} = \frac{1}{eF_o} = \frac{2\lambda}{\sqrt{3}\mu e}. \quad (3.21)$$

By comparing this with  $R_{max}$ , we get,

$$\alpha \geq \frac{3}{4} \Rightarrow \xi \geq R_{max}. \quad (3.22)$$

We see that the results in this section are valid only in the regime where the penetration length is greater than the radius. In this regime, the charge distribution is roughly uniform being only slightly enhanced near the surface of the Q-ball.

We conclude this section by considering the potential Eqn.(3.10) with  $\lambda^2 = 3/16$ . As we now show, in this case  $\xi \ll R_{max}$  and the Q-ball is superconducting. For this case,  $\alpha = 0$  and the "false" vacuum ( $F = F_o = 2\mu$ ) is degenerate with the "true" vacuum ( $F = 0$ ). The potential energy is therefore zero inside as well as outside of the Q-ball and is non-zero only in the shell in which  $F$  changes from  $2\mu$  to 0. Let  $T$  be the thickness of this shell and  $R$  be the radius of the Q-ball. From Eqn.(2.11) we find the following approximate expression for the energy:

$$E \simeq \frac{8\pi\mu^2 R^2}{T} + \frac{e^2 Q^2}{8\pi R} \left( 1 + \frac{x^2 A(x)}{2} \right) + \pi R^2 T \mu^4 \quad (3.23)$$

where

$$A(x) = \left( \frac{\tanh x}{x - \tanh x} \right)^2 \left( \frac{1}{x \tanh x} - \frac{1}{\sinh^2 x} \right) \quad (3.24)$$

Eqn.(3.23) deserves some explanation. First, we note that each of the terms in this expression is accurate only up to numerical factors of order unity. The first term is the scalar gradient term where we have set  $f' = F_o/L = 2\mu/L$ . The second and third terms are the Coulomb and  $f^2g^2$  terms respectively. The last term is the potential energy in the shell where the average energy density in the shell is taken to be  $\mu^4/4$ .

Minimizing the energy with respect to  $T$  we find that  $T = 2\sqrt{2}\mu^{-1}$ . Substituting this into Eqn.(3.23) we find an expression for  $E$  in terms of  $R$  and  $Q$ . Let us now assume that  $x \gg 1$ . We will check this assumption at the end of the calculation. For  $x \gg 1$  we find that  $A(x) \simeq x^{-3}$  and

$$E \simeq 4\sqrt{2}\pi\mu^3R^2 + \frac{e^2Q^2}{8\pi R} \left(1 + \frac{1}{2x}\right). \quad (3.25)$$

Minimizing this expression with respect to  $R$  we find that

$$R = \frac{2^{-1/6}}{\mu} \left(\frac{eQ}{8\pi}\right)^{2/3} \quad (3.26)$$

and

$$\frac{E}{\mu} = \frac{3}{2^{11/6}\pi^{1/3}} (eQ)^{4/3}. \quad (3.27)$$

where we have only used the leading order terms. As before, we find  $Q_{max}$  by solving  $\partial E/\partial Q = \mu$ . We obtain

$$Q_{max} = \frac{\pi}{\sqrt{2}e^4} \quad (3.28)$$

For weak couplings this can be quite large.

Eqns.(3.23-3.28) are valid only for  $x \gg 1$  and we must check that this is indeed the case. For  $Q = Q_{max}$ ,  $x = (2\sqrt{2}e)^{-1}$ , which is indeed greater than one for weak ( $e < 2^{-3/2}$ ) coupling. For stronger couplings or for smaller  $Q$  the large  $x$  approximation breaks down.

Finally, we compare the size of these Q-balls to the penetration length. From Eqn.(3.26) we see that

$$R|_{Q=Q_{max}} = \frac{1}{4\sqrt{2}\mu e^2} \quad (3.29)$$

This is greater than the penetration length  $\xi = 1/(e\mu)$  for weak ( $e < 1/(4\sqrt{2})$ ) coupling. It is in this limit that the interior of the Q-balls becomes superconducting. From Eqn.(3.1) it is easy to see that the charge density at the center of the Q-ball is  $\mathcal{O}(e^{-x})$  of the charge density near the surface and the width  $T$  of the shell in which most of the charge resides is of order  $(eF)^{-1} \sim (m_V)^{-1}$  as expected for a lump of superconductor.

## 4 Numerical Results

In this section we present numerical solutions of gauged Q-balls. These results are used to 1) verify the general properties of gauged Q-balls derived in Section II; 2) check the accuracy of the thin wall approximation; and 3) explore properties of gauged Q-balls that cannot be studied in the thin wall approximation.

The thin wall approximation discussed above is applicable to a rather limited set of Q-balls. Specifically, the results of Section III are valid for Q-balls in which the surface energy is small compared to the volume energy (i.e., the radius of the Q-ball is large compared to the thickness of the shell within which  $f$  changes from  $F$  to 0). However, for large values of  $e$  Q-balls have a maximum size that is small, so surface energies are always important. Moreover, many of the results in Section III assume that  $x \ll 1$  where  $x$  is given in Eqns.(3.18,3.19). This, for example, implies that the equations for  $Q_{max}$  are valid only for certain values of  $\lambda$ . Because of the limitations of the thin shell analysis (the only analytical approach that we found tractable) the numerical analysis for gauged Q-balls is particularly important.

Consider the Lagrangian Eqn.(2.8) with the potential given in Eqn.(3.10). We scale the dimensionful quantities  $f, g$ , and  $r$  by appropriate factors of  $\mu$ . In order to keep the notation simple, we use the same symbols for the dimensionless quantities in this section as we did for the dimensionful quantities in the previous sections (e.g.,  $r$  here is equal to  $r/\mu$  of Sections II and III). For physical quantities such as  $E$ , we write the factors of  $\mu$  explicitly.

From the Lagrangian and the potential we get the equations of motion

$$\frac{1}{r} \frac{\partial^2}{\partial r^2}(rf) = -g^2 f + (\lambda^2 f^5 - f^3 + f) \quad (4.1)$$

$$\frac{1}{r} \frac{\partial^2}{\partial r^2}(rg) = e^2 g f^2 \quad (4.2)$$

with the charge and the energy given by

$$Q = 4\pi \int dr r^2 g f^2 \quad (4.3)$$

$$E = 4\pi\mu \int dr r^2 \left[ \frac{1}{2}(f')^2 + \frac{1}{2e^2}(g')^2 + \frac{1}{2}f^2 g^2 + \left( \frac{1}{6}\lambda^2 f^6 - \frac{1}{4}f^4 + \frac{1}{2}f^2 \right) \right]. \quad (4.4)$$

As discussed above, a finite energy Q-ball solution must satisfy  $f'(0) = g'(0) = 0$  and  $g(\infty) < 1$ . Furthermore, a Q-ball solution with minimum energy for a given charge will be non-oscillatory (zero node solution).

To find acceptable Q-ball solutions we numerically integrate Eqns.(4.1,4.2) from  $r = 0$  to  $r = \infty$  (or rather, to a point well outside the Q-ball, i.e., where  $f \simeq 0$ ). [Recall that we required  $\lambda^2 > 3/16$  so that  $U(f) > 0$  for all  $r$ .] Eqns.(4.1,4.2) are equivalent to a system of four first order differential equations. In order to find Q-ball solutions, we must determine the boundary conditions (i.e., the values of  $f, g$  and their first derivatives at  $r = 0$ ). We know that  $f'(0) = g'(0) = 0$ . Fixing  $g(0)$  determines the charge.  $f(0)$  is then adjusted to give a non-oscillatory solution with  $f(r) \rightarrow 0$  for  $r \rightarrow \infty$ . [For definiteness, we choose  $f(0) > 0$ .]

Let us be more specific. For a given choice of  $f(0)$ ,  $f(r)$  will (1) grow without bound, (2) become negative for some  $r$ , (3) change from a decreasing to an increasing function of  $r$ , or (4) go smoothly to 0 as  $r \rightarrow \infty$ . Note that the gauged case differs from the ungauged case in that  $f(r)$  can begin as an increasing function of  $r$  and then turn over and go smoothly to zero at infinity.

In practice, a value of  $f(0)$  is selected, and the solution is integrated out until it becomes clear which of the four types it belongs to. 1 or 2 type solutions indicate that  $f(0)$  was too big while type 3 solutions indicate that  $f(0)$  was too small. The value of  $f(0)$  is appropriately adjusted and the process is repeated until the desired accuracy is obtained. The value of  $g(\infty)$  must then be checked to make sure it is less than 1. In Fig.1 we plot  $f(r)$  and  $g(r)$  as a function of  $r$  for a gauged Q-ball with  $e^2 = 0.01$  and  $Q \simeq 10^4$

For comparison, we show on the same plot  $f(r)$  and  $\omega$  for an ordinary ( $e = 0$ ) Q-ball of roughly the same charge. Note that  $g(r)$  is a monotonically increasing function of  $r$  as is expected from Eqn.(2.15). In Fig.2, we plot the charge density  $\rho(r) \equiv 2gf^2$  as a function of  $r$  for the gauged and ordinary Q-balls in Fig.1. While charge is distributed uniformly inside the ordinary Q-ball, the charge is pushed towards the surface of the gauged Q-ball. Note also that the radius of the configuration has grown compare to the  $e = 0$  case. In Fig.3, we plot  $E/\mu Q$  as a function of  $Q$  for various values of  $e$ . The unstable regions discussed in the text, those where  $\partial E/\partial Q > \mu$  are now apparent. Note that as we increase



the value of  $e^2$ , the instability occurs for smaller values of  $Q$ . We also see that the slope for the  $e = 0$  case never changes sign, indicating the absence of an instability for ordinary  $Q$ -balls. In Fig.4 we plot  $f(r)$  and  $g(r)$  for a  $Q$ -ball configuration using  $\lambda^2 = 0.64$  and  $e = 0.01$ . The charge for the configuration is 88,921. For comparison, we show the  $f(r)$  and  $g(r)$  used in the thin shell approximation. This indicates that the analytic ansatz used is not too far off. Finally, as mentioned above, there exists a value of  $e$  ( $\equiv e_{crit}$ ) above which  $Q_{max} < Q_{min}$ . For  $e > e_{crit}$  there are no stable  $Q$ -balls. In Fig. 5. we plot  $e_{crit}$  as a function of  $\lambda$ .

## 5 Gauged Nontopological Solitons with Fermions

The work presented above can easily be extended in a number of ways. The one we chose was to add Fermions to the previous model. Here we study nontopological solitons that occur when charged fermions are trapped inside a region of false vacuum[7]. Consider a theory with a real scalar field  $\sigma$  and Dirac fermion field  $\psi$ . The scalar potential is taken to be

$$V = \frac{1}{2}\mu^2\sigma^2 \left(1 - \frac{\sigma}{\sigma_0}\right)^2 \quad (5.1)$$

where we assume that  $\sigma = 0$  is the true vacuum and  $\sigma = \sigma_0$  is the false vacuum. The Lagrange density for  $\psi$  is

$$\mathcal{L}_\psi = i\bar{\psi}\gamma^\mu(\partial_\mu + ieA_\mu)\psi - m\left(1 - \frac{\sigma}{\sigma_0}\right)\bar{\psi}\psi \quad (5.2)$$

so that  $\psi$  has mass  $m$  in the true vacuum and is massless in the false vacuum.

The case where  $e = 0$  was considered by Lee and Pang[7] and we briefly review their results before turning to the gauged case. Suppose there are  $N$   $\psi$  particles trapped in a spherical region of false vacuum. The energy for the configuration is

$$E \simeq \frac{3\pi}{4} \left(\frac{3}{2\pi}\right)^{2/3} \frac{N^{4/3}}{R} + \frac{2\pi}{3}\mu\sigma_0^2 R^2. \quad (5.3)$$

The first term is the fermi energy for the  $\psi$  particles while the second term is the energy in the surface of the soliton. [For the potential Eqn.(5.1) the false vacuum is degenerate with the true vacuum and so there is no volume term in the expression for the total energy.]

For fixed  $N$  the energy is minimized by choosing

$$R = \left[ \frac{9}{16} \left( \frac{3}{2\pi} \right)^{2/3} \frac{N^{4/3}}{\mu\sigma_o^2} \right]^{1/3} \quad (5.4)$$

At this radius, the energy of the soliton is given by:

$$E = \frac{3}{4} \left( \frac{3^7\pi^5}{2} \right)^{1/9} (\mu\sigma_o^2)^{1/3} N^{8/9}. \quad (5.5)$$

As discussed in [7], since the exponent of  $N$  is less than 1, solitons with large enough  $N$  will have energy less than  $N$  free  $\psi$  particles and will therefore be stable against dispersion. More precisely, for  $N > (3^{16}\pi^5/2^{19})(\mu\sigma_o^2/m^3)^3$ ,  $E < Nm$  and the solitons would be stable against dispersion into free particles.

Suppose now that the fermions are coupled to a  $U(1)$  gauge field  $A_\mu$  as in Eqn.(5.2). The energy will be then given by Eqn.(5.3) plus a Coulomb term  $\beta e^2 N^2/R$  where  $\beta$  is a number of order  $10^{-1}$  that depends on the charge distribution of the fermions. [For a uniform charge distribution,  $\beta = 3/20\pi$ .] Again, we keep  $N$  fixed and minimize the energy with respect to  $R$ . We find that

$$R = \left[ \frac{3}{4\pi} \frac{1.44N^{4/3} + \beta e^2 N^2}{\mu\sigma_o^2} \right]^{1/3} \quad (5.6)$$

and

$$E = \left( \frac{9\pi\mu\sigma_o^2}{2} \right)^{1/3} (1.44N^{4/3} + \beta e^2 N^2)^{2/3} \quad (5.7)$$

For stable solitons to exist,  $E < mN$  for some range of values of  $N$ . Clearly, this depends on  $e$ , the ratio  $\mu\sigma_o^2/m^3$  and  $\beta$ .  $e$  and  $\mu\sigma_o^2/m^3$  are model dependent parameters.  $\beta$  on the other hand, depends on the structure of the soliton and must be determined by explicitly solving for the soliton configuration. However, the exact value of  $\beta$  is not necessary for the present discussion.

In Fig. 6 we show  $E/Nm$  against  $N$  for two representative choices of  $e$  and  $\mu\sigma_o^2/m^3$  [one in which stable solitons exist and the other in which they do not] and take  $\beta = 0.048(\simeq 3/20\pi)$ . We see that fermion NTSs can occur even when the fermions are coupled to a  $U(1)$  gauge field. As with gauged Q-balls there is a maximum charge. Furthermore, in certain theories (c.f. example 2 in fig. 2) stable NTSs do not exist at all

## 6 Summary and Discussion

Solitons, whether topological or nontopological, may be interesting for cosmology as well as particle physics. The cosmological implications of topological solitons such as domain walls, cosmic strings and magnetic monopoles have been studied for some time. On the other hand, the cosmological significance of nontopological solitons has been considered only recently. The discovery of a relic abundance of NTSs would be clear evidence for a phase transition in the early Universe and therefore have important implications for particle physics. Moreover, NTSs are potential candidates for the dark matter in galactic halos [5]. It is therefore of great interest to explore the possible particle physics theories in which NTSs might arise.

NTSs occur in theories with a continuous symmetry and therefore a conserved Noether charge. Previous investigations of NTSs have, for the most part, concentrated on theories with *global* symmetries. However, many of the theories that we know of (or at least believe in) involve gauge or *local* symmetries. In this work, we have considered NTSs (Q-balls) in the simplest gauge theory; namely, one with a local  $U(1)$  symmetry.

For fixed charge, the NTS is the groundstate configuration. Stability against dispersion into free particles is demonstrated by computing the energy of a soliton solution of charge  $Q$  and comparing this with the energy of  $Q$  free particles. Stability against fission, evaporation of charge from the surface [6,8], and gravitational collapse must also be checked [9]. The existence of *stable* NTSs therefore depends on particle physics phenomenology such as the shape of the scalar potential or the coupling of scalars to fermions. This is in contrast to topological solitons where existence and stability are determined from the symmetry breaking pattern of a given theory [e.g., stable vortices or cosmic strings occur in any theory in three spatial dimensions in which a  $U(1)$  symmetry is spontaneously broken].

Coleman [4](see also Rosen [3]) has demonstrated the existence of stable NTSs or Q-balls in a theory with a single complex scalar field and a global  $U(1)$  symmetry. We have considered a similar model but with a local  $U(1)$  symmetry and find that gauge interactions affect the structure and stability of the Q-ball in a physically intuitive way. For small gauged Q-balls ( $R \ll m_{\tilde{\nu}}^{-1}$ ) the configuration is perturbed only slightly from

ORIGINAL PAGE IS  
OF POOR QUALITY

the  $e = 0$  case with a small charge enhancement near the surface of the Q-ball. For larger Q-balls ( $R \gg m_V^{-1}$ ) most of the charge is distributed at the surface. This is consistent with the fact that the interior of the Q-ball is superconducting. Furthermore, there is a maximum size for stable Q-balls which occurs once the Coulomb barrier becomes too large. Finally we recall an important difference with the  $e = 0$  case; the fact that it is impossible to have gauged Q-matter.

**Acknowledgments :**

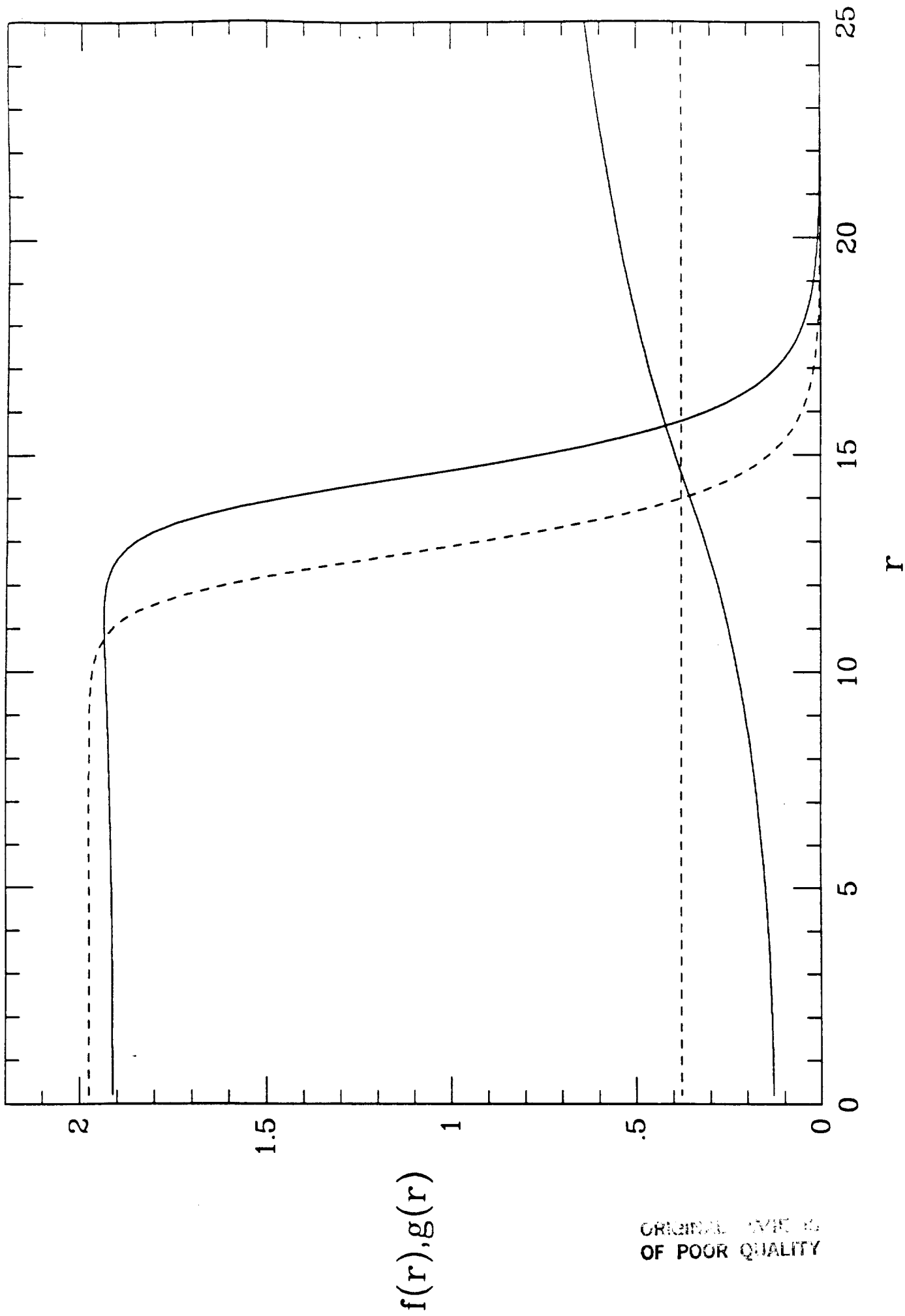
We wish to thank Marcelo Gleiser for many useful discussions. RW wishes to thank M.Srednicki for continued encouragement and support. This work was supported in part by the DoE (at Chicago and Fermilab) and NASA (at Fermilab). LW acknowledges the financial support of the NASA Graduate Student Researchers Program. The work of RW was supported in part by NSF Grant No. PHY-86-14185.

### Figure Captions

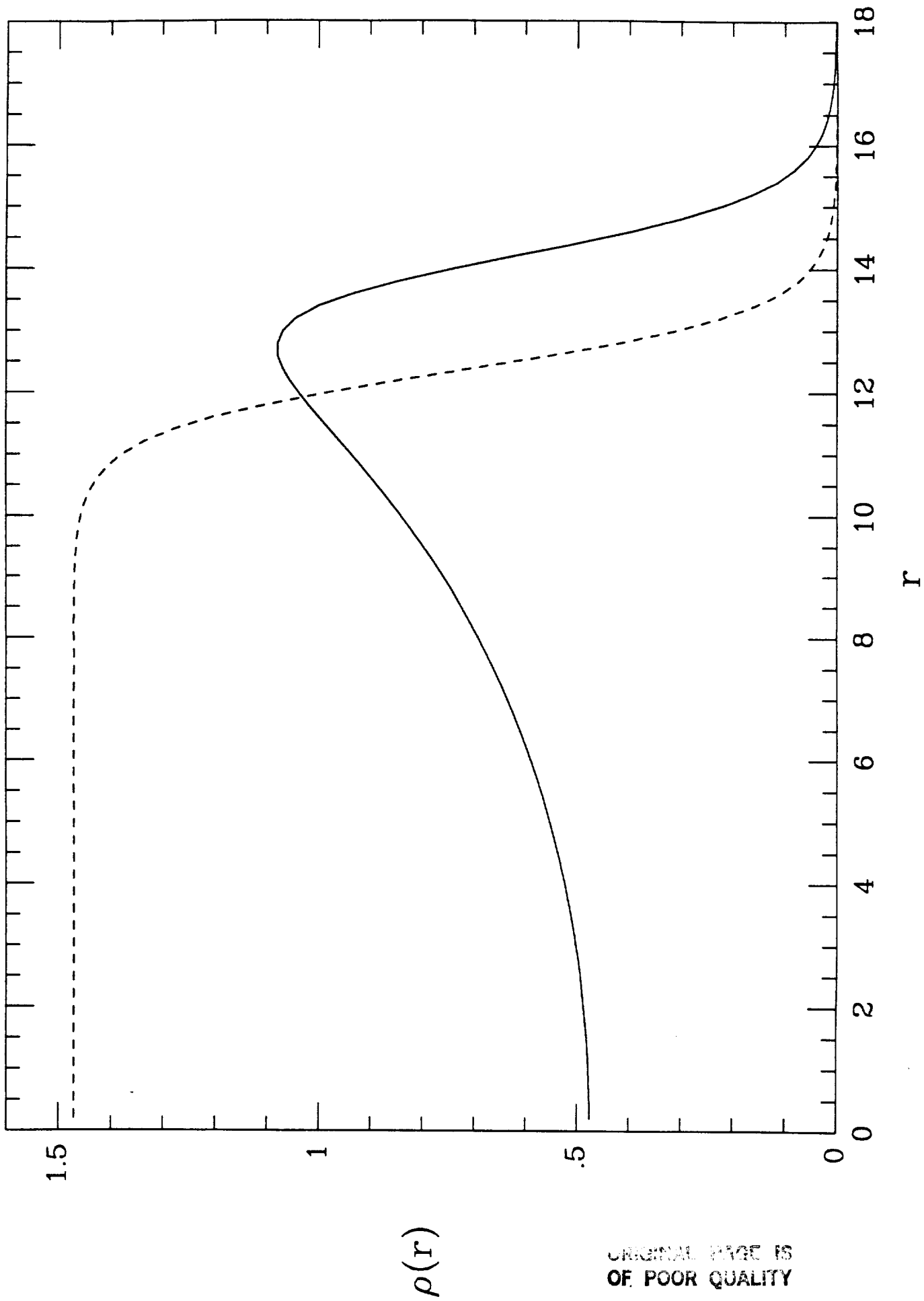
- Fig.1 Plot of the scalar field  $f(r)$  and the gauge field  $g(r) \equiv \omega - eA_0$  as a function of  $r$ . The solid lines are for  $e^2 = 0.01$  with  $Q = 11,119$ . The dashed lines are for  $e = 0$  with  $Q = 10,941$ . For both cases, we have set  $\lambda^2 = 0.2$ .
- Fig.2 Plot of the charge density  $\rho(r) \equiv 2gf^2$  as a function of  $r$  for the two field configurations plotted in Fig.1. Notice that in the gauged case, the charge accumulates at the boundary of the Q-ball.
- Fig.3 Plot of  $E/\mu Q$  as a function of  $Q$  with  $\lambda^2 = 0.20$  for various values of  $e$ .
- Fig.4 Plot of  $f(r)$  and  $g(r)$  (solid lines) for a Q-ball configuration with  $\lambda^2 = 0.64$  and  $e^2 = 10^{-4}$ .  $Q$  for the configuration shown is 88,921. The dashed lines are the corresponding  $f(r)$  and  $g(r)$  used in the thin wall approximation.
- Fig.5 Plot of  $e_{crit}$  as a function of  $\lambda$ . As discussed in the text, for  $e > e_{crit}$  there are no stable Q-balls as  $Q_{max}$  is less than  $Q_{min}$ .
- Fig.6  $E/mN$  as a function of  $N$  for the fermion ball.

References

1. T.D.Lee, Phys. Rep., **23C**, 254 (1976).
2. R.Friedberg, T.D. Lee and A Sirlin, Phys. Rev. **D10** ,2739 (1976).
3. G. Rosen, J. Math. Phys. **9**, 996 and 999 (1968).
4. S. Coleman, Nucl. Phys. **B262**, 263 (1985).
5. J.A. Frieman, G.B. Gelmini, M. Gleiser and E.W.Kolb, Phys. Rev. Lett. **60**, 2101 (1988).
6. A. Cohen, S.Coleman, H. Georgi and A. Manohar, Nucl.Phys **B272** (1986) 301.
7. T.D. Lee and Y. Pang, Phys. Rev. **D35** (1987),3678.
8. A. M. Safian and S.Coleman, Nucl. Phys **B297** (1988) 498.
9. M.Gleiser Fermilab-Pub-88/67-A  
Ph. Jetzer Fermilab-Pub-88/66-A.

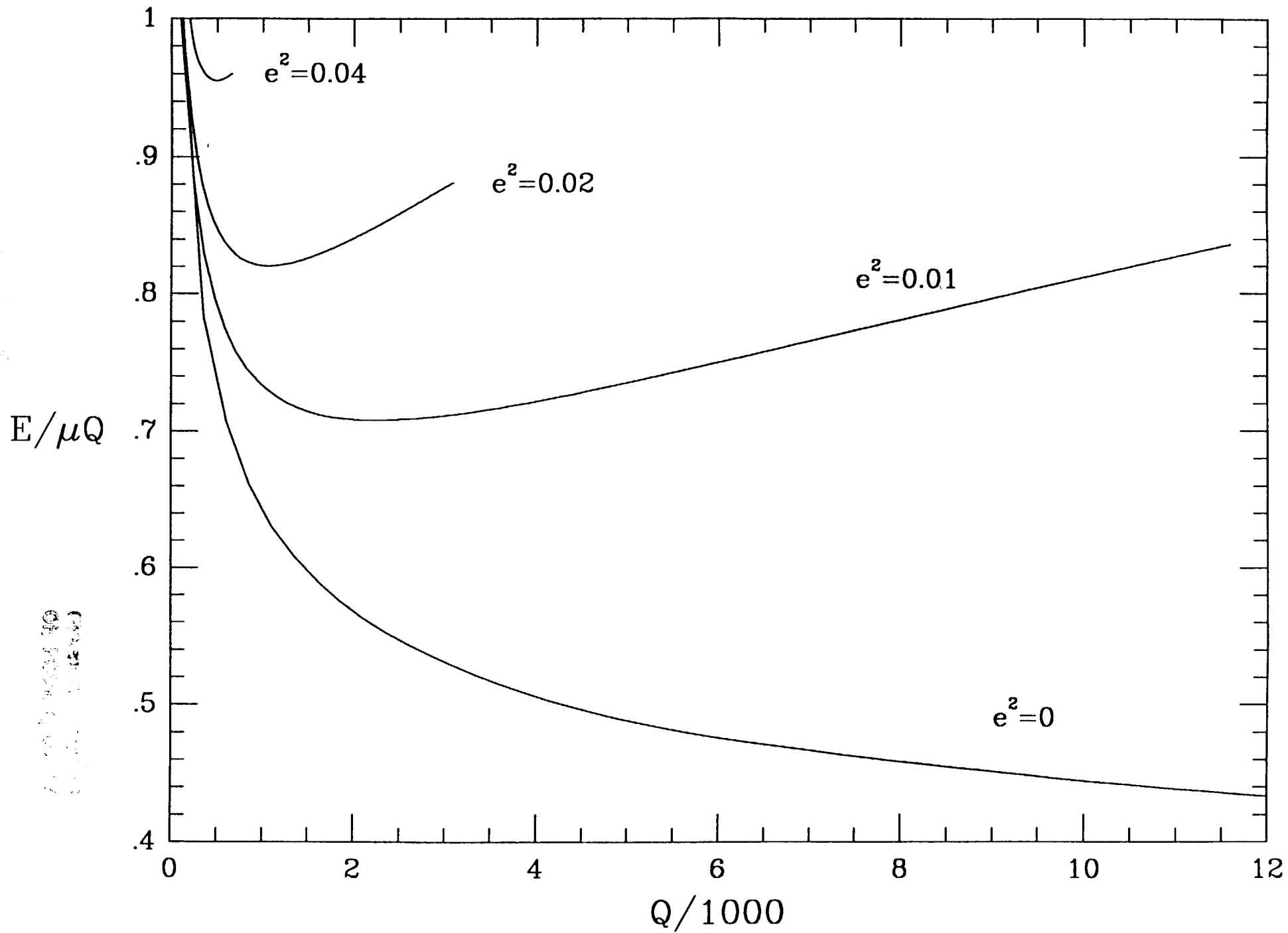


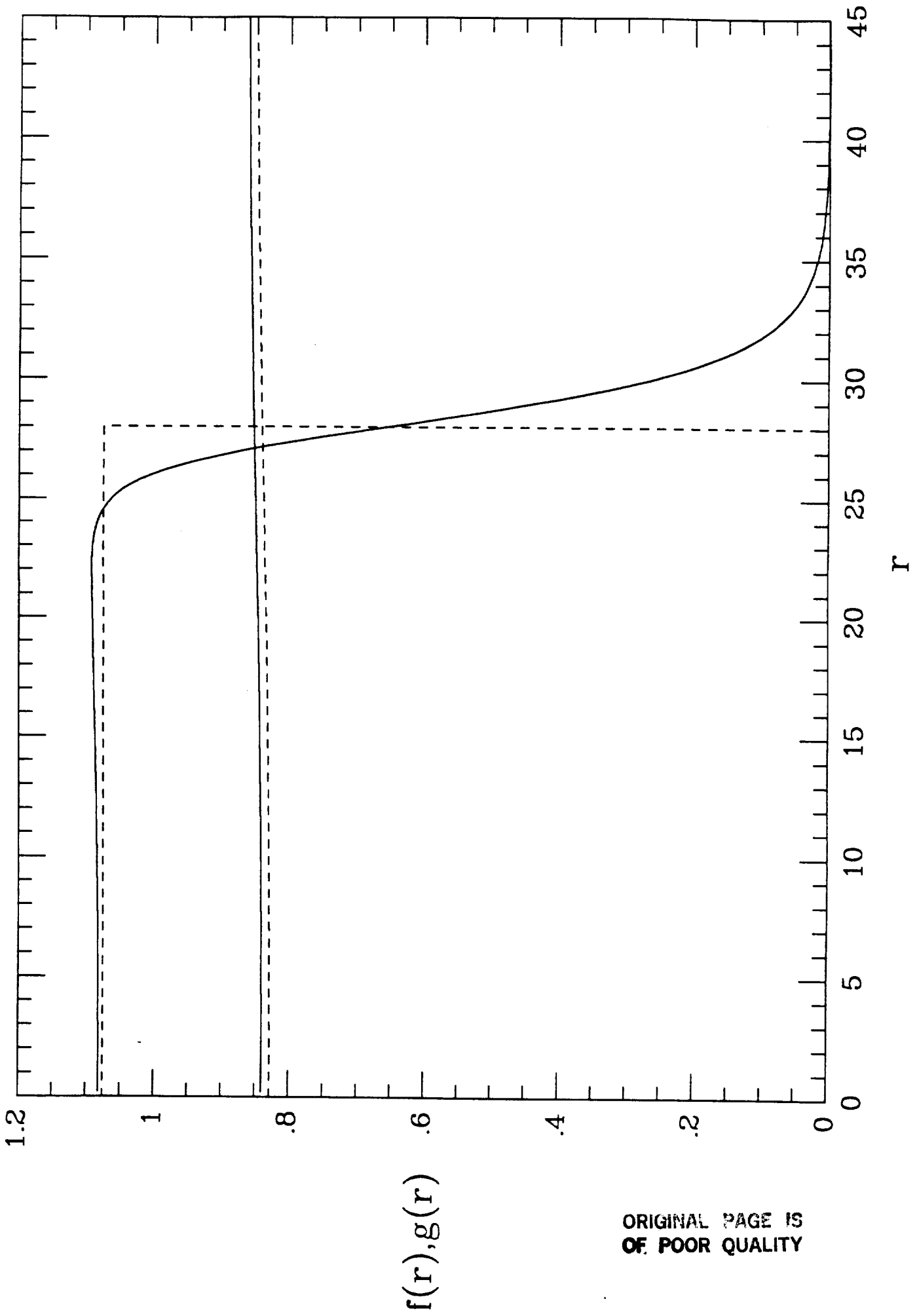
ORIGINAL IMAGE IS  
OF POOR QUALITY



ORIGINAL PAGE IS  
OF POOR QUALITY







ORIGINAL PAGE IS  
OF POOR QUALITY